

Early Stages of Fischer–Tropsch Activity on ThO_2 and $\text{Th}_{0.9}\text{Ce}_{0.1}\text{O}_2$

Alexis Grabbe and Richard C. Jarnagin*

Department of Chemistry, CB #3290, The University of North Carolina at Chapel Hill, Chapel Hill, NC 27599, USA

The early stages of CO hydrogenation catalysed by high-purity high surface area thorium oxide and cerium-doped thorium oxide have been examined in the 15–20 Torr range in an attempt to find the intrinsic factors that influence the Fischer–Tropsch (FT) activity of these robust materials. The surfaces of the clean oxide powders were characterized by gas–solid oxygen isotope exchange over an O_2 pressure range of 1–4 Torr. Doping with cerium significantly enhanced the exchange rate, causing a lowering of 40 kJ mol^{-1} of the activation energy for both atomic (single O atom) and molecular (double O atom) exchange mechanisms relative to the same exchange processes on pure thoria.

The initial product distribution obtained at very low conversions of CO at 685 K and 15–20 Torr total pressure over the two materials indicates that the cerium-doped material makes alkenes preferentially over alkanes. Neither catalyst was found to generate oxygenated hydrocarbons as earlier reported. The shift in product distribution obtained over doped thoria ($\text{Th}_{0.9}\text{Ce}_{0.1}\text{O}_2$) compared with that obtained over pure thoria was consistent with the redox chemistry of cerium and an assumed enediolate intermediate. The product distribution obtained over doped oxide was accompanied by a threefold increase in the rate of consumption of CO with respect to the rate obtained over pure thoria. The rate increase correlated positively with the change in rate of oxygen exchange. A significant induction period was observed over both catalysts. Such early-stage delays have not previously been reported for this system.

Fischer–Tropsch processes may be broadly considered as any heterogeneously catalysed hydrogenation of CO by H_2 to form aliphatic and oxygenated hydrocarbons. In this work, clean vacuum techniques were used to examine early stages of the FT process on high-purity powdered oxides to bridge the gap between ultra-high vacuum single-crystal studies and high-pressure developmental studies. The intent was to connect early-stage products to early-stage surface chemistry before later-stage processes could reform initial products and surfaces. Thoria was selected as a catalyst for various reasons. It was a component of the original FT standard catalyst¹ and it has robust resistance to sulphur.¹ It has been reported to have unusual properties with regard to alcohol synthesis and isosynthesis^{1,2} and a significant body of IR spectroscopic evidence has accumulated regarding surface complexes formed on it.^{3,4,5} Additionally, a significant amount of thorium substances have accumulated as by-products from nuclear processing.

Fast, sensitive, and accurate mass spectrometric acquisition methods were developed for conduct of the measurements at low pressure over powders.⁶ These methods were applied quantitatively to oxygen isotope exchange between gas and solid oxides as a means for the *in situ* characterization of the surfaces of pristinely clean oxides. By these methods the role of oxygen vacancies on the solid can be estimated and the changes in oxygen lability brought about by doping with substituent ions can also be determined.

Cerium ion was selected as dopant ion because it goes into the thoria fluorite lattice substitutionally⁷ and because its $3^+/4^+$ redox chemistry was speculated to enhance oxygen exchange through vacancy formation on the oxide surface.

The characterized oxides were used to execute low-pressure synthesis from CO– H_2 mixtures. The product distributions were observed with time as they depend on changing catalyst composition at fixed lattice type. The results are discussed with respect to the redox chemistry of cerium, a mechanism for carbon–carbon bond building proposed by Mazanec,⁸ and the conditions necessary for alcohol synthesis proposed

by Frost.⁹ The present results and redox interpretation are consistent with recent results obtained on pure ceria by Arai *et al.*¹⁰

Experimental

Materials

Thorium oxalate was prepared by precipitation with stoichiometric amounts of oxalic acid from the aqueous nitrate dissolved in $17 \text{ M}\Omega \text{ cm}$ organic-free water.^{11,12} This procedure maximized exclusion of non-thorium metal ions, *e.g.* those of iron, nickel and copper as well as alkali-metal and alkaline-earth metal ions. The oxalate was calcined at 890 K for 16 h in flowing oxygen while contained in a high-purity boat and tube of silica (low sodium silica for electronics fabrication). The pure oxide had a B.E.T. surface area of $17.8 \text{ m}^2 \text{ g}^{-1}$. Preparation of $\text{Th}_{0.9}\text{Ce}_{0.1}\text{O}_2$ was by co-precipitation of a solution of thorium nitrate and cerium (iv) ammonium nitrate with oxalic acid, followed by calcining as above. The resulting oxide had a B.E.T. area of $33 \text{ m}^2 \text{ g}^{-1}$. Care was taken to ensure that additional metallic contaminants were not introduced into the oxides. The cerium (iv) ammonium nitrate $[\text{Ce}(\text{NH}_4)_2(\text{NO}_3)_6 \cdot 2\text{H}_2\text{O}]$ was obtained from Johnson Matthey, the thorium nitrate $[\text{Th}(\text{NO}_3)_4 \cdot 4\text{H}_2\text{O}]$ was obtained from Mallinckrodt, St. Louis, MO, USA, and the oxalic acid $[\text{H}_2\text{C}_2\text{O}_4 \cdot 2\text{H}_2\text{O}]$ was obtained from EM Science, Cherry Hill, NJ, USA. In the worst case total quantities of metallic impurities in the oxides did not exceed 72 ppm. In particular, nickel and copper were present at < 1 ppm and iron was present in 10–20 ppm concentrations. These low levels should ensure low concentrations of supported 3d–4d metal atoms exposed by the reducing FT atmosphere. Post-catalysis surface analysis by SIMS and volume analysis by atomic emission spectroscopy[†] found iron at 20–40 ppm and 21–31 ppm, respectively, and nickel and copper at < 1 ppm. These levels indicate that the oxides were not contaminated progressively during CO reductions, and are consistent with the storage and manipulation of CO in

† 1 Torr = $101\,325/760$ Pa.

‡ Atomic Emission Analysis kindly supplied by Dr. John Olesik.

non-metallic vessels after purification. O¹⁸-enriched dioxygen (90–96 atom%) was obtained from Cambridge Isotopes.

Gas reaction mixtures were prepared on an LN₂ trapped and oil diffusion pumped glass vacuum system. Hydrogen (99.9997%) and Neon (99.999%) from Matheson Gas Products, East Rutherford, NJ, USA, were used without additional purification. Carbon monoxide (99.99%) from Matheson, was passed over a hot (470 K) molecular sieve to decompose metal carbonyls and trap the metals formed. The metal-carbonyl-free CO was stored in glass vessels fitted with Teflon valves. The CO and its feedstocks were in contact with metal-containing devices for only a few minutes during pressure measurements and mixing operations. Thus precautionary steps were taken at each stage, both wet chemical and gas manipulation, to ensure that observed catalytic activity would be attributable to high-purity oxides. Because a zeolite sieve was used during decomposition of metal carbonyls, some hydrocarbon impurities and CO₂ at ppm levels were unavoidably injected into the feed mixtures. The contribution from the hydrocarbons was subtracted from the amounts generated by oxide-based catalytic processes. Mixtures of 2 : 1, 2.5 : 1 and 3 : 1 H₂ : CO were prepared, each with an additional 1–4% of neon added as a tracer gas for normalisation of signals from the mass spectrometer.

Methods

The analysis mass spectrometer was a UTI 100C gas analyser, mounted in a separate chamber attached to the reactor through a sampling capillary. The analyser chamber was continuously pumped by a 50 dm³ s⁻¹ turbomolecular pump up to 3 × 10⁻⁹ Torr. The magnitude of mass-spectrometric signals from background gases in this chamber fluctuated <5% over periods of 8 h. The mass spectrometer was connected downstream from the reactor via a silica capillary leak and an all-metal metering valve. The 200 cm³ main reactor was constructed from electronics-grade silica with thermocouple wells. The reactor lay in a tube furnace that was computer controlled to ±0.5 °C over the longest reaction time period. The reactor was also connected through greaseless valves to a glass gas manifold with associated gas reservoirs and pressure gauges. The manifold was connected to a cold-trapped (freon) diffusion pump through greaseless metal valves. The pressure in the reactor was measured with a capacitance manometer at the start and finish of each experiment. The minimum pressure attainable in the reactor was in the low 10⁻⁸ Torr range. The system was monitored and controlled through a Data Translation DT2821 50 KHz acquisition card and IBM-AT computer. The acquisition and analysis software was written in ASYST.† The reactor and interconnect system had a mass-spectrometrically-measured response time (0–95%) to oxygen isotope compositional changes of 20 s. The mass spectrometer multiplexing of 60 mass numbers and the accommodation of multiplier electrodes to multiple species slowed the overall system response to several minutes during CO conversion runs. Oxygen-exchange data were corrected for time-dependent detector gain through appropriate normalisation, including time-dependent multiplier gain, mass-dependent gain, and mass-dependent transport factors. Hydrocarbon spectra were normalised to tracer gas (Ne) signals, and were decomposed into individual cracking patterns for each species by a least-squares method.

Prior to oxygen-exchange experiments, samples of catalyst (0.15–0.3 g) were treated with alternating evacuations to ultra-high vacuum and roasting in 3–10 Torr of naturally dis-

tributed O₂ at reaction temperature. This treatment ensures removal of uncontrolled densities of water and carbonaceous materials from the oxide surfaces. These steps were repeated until the reactor could be evacuated to 10⁻⁸ Torr within 5 min of an oxygen treatment. Prior to FT experiments, a catalyst cleaned in the above manner was treated by repeated cycles of exposure to synthesis gas at reaction temperature followed by evacuation to less than 1 × 10⁻⁵ Torr. Three to four repetitions were necessary for the catalytic properties to become reproducible for that composition of make-up gas. This treatment added water and carbonaceous materials to the surfaces in a quasi-equilibrated fashion.

There are three classes of distinguishable isotope-exchange reactions¹³ for O¹⁸-enriched gaseous oxygen exchanging with an unenriched metal oxide. Pure single-atom exchange between gas-phase dioxygen and lattice oxygen atoms (ions) is called an R1 process. Pure dioxygen exchange between gas and pairs of lattice oxygen is called an R2 process. Exchange between gas-phase molecules, but not with the lattice, catalysed by the surface is designated as an R3 process. These processes are representable as a set of seven coupled ordinary differential equations containing three adjustable rate constants *k*₁, *k*₂ and *k*₃. The equations have been solved analytically to give the time dependence of the partial pressures of the gas-phase isotopic species.^{13,14}

Results

Oxygen Exchange

Oxygen exchange experiments over both catalysts were performed between 680 and 774 K. Typical data are shown in Fig. 1. It was found when fitting curves of gas-phase oxygen isotope composition vs. time for both ThO₂ and Th_{0.90}Ce_{0.10}O₂ that *k*₃ was always small and negative, an unphysical result. Curves were fitted only for *k*₁ and *k*₂ therefore, and surface-catalysed exchange between molecular species from the gas (*k*₃) was assumed not to occur. Reports of non-zero *k*₃ are rare.^{14,15}

The observed rate constants as a function of temperature were fitted to an Arrhenius expression. Fig. 2 displays plots for *k*₁ and *k*₂ over pure ThO₂ and over Th_{0.9}Ce_{0.1}O₂, respectively. The fitted results are given in Table 1.

The results for pure thoria and Winter's¹⁴ results are in good agreement considering the disparity between the equipment available to him and the present experimental arrangement as well as the difference in the temperature/pressure regime over which the results were taken.

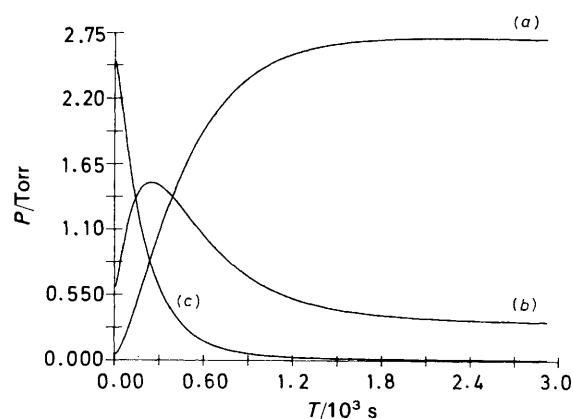


Fig. 1 Oxygen isotope exchange, O¹⁸-enriched gas–natural O ThO₂, area, 4.75 m²; *T* = 712 K. The curves are unsmoothed data recorded at intervals of 3 s per point. Each recorded point results from signal averaging of 60 values (a) oxygen 16–16; (b) oxygen 16–18; (c) oxygen 18–18

† Adaptable Laboratory Software, Rochester, New York.

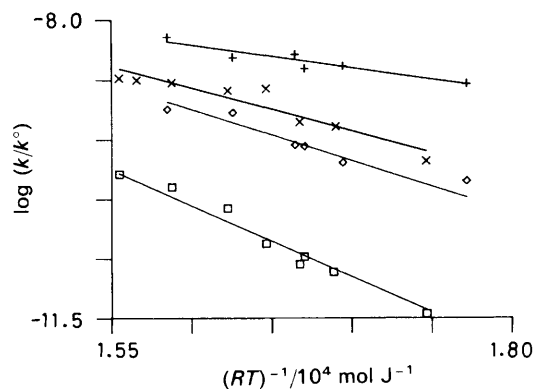


Fig. 2 Temperature dependence of oxygen exchange. \times , $+$, single-atom exchange; \square , \diamond , double-atom exchange; \times , ThO_2 , $E_a = 83.3$ kJ mol $^{-1}$; $+$, $\text{Th}_{0.9}\text{Ce}_{0.1}\text{O}_2$, $E_a = 44.0$ kJ mol $^{-1}$; \square , ThO_2 , $E_a = 137$ kJ mol $^{-1}$; \diamond , $\text{Th}_{0.9}\text{Ce}_{0.1}\text{O}_2$; $k^\circ = 1$ mol exchange Torr $^{-1}$ m $^{-2}$ s $^{-1}$

An interesting comparison can be made in the number of surface layers participating in the exchange. Winter¹⁴ reported the amount of exchangeable oxygen (n_{ex}) in ThO_2 as 5–11 times the number of oxygens present in one surface layer as determined by the B.E.T. method. By the same measure, for CeO_2 , he reported $n_{\text{ex}} = 4$ –5 layers. From the present data we find $n_{\text{ex}}(\text{ThO}_2) = 14$, while $n_{\text{ex}}(\text{Th}_{0.9}\text{Ce}_{0.1}\text{O}_2) = 9$ layers. The decrease in the number of exchangeable oxygens in the Ce-doped material may be ascribed to a relatively slower rate of diffusion into the surface layer. Note that the current data indicate that measurable diffusion does not occur from the bulk in the case of ThO_2 . However, bulk diffusion appears to be detectable, although not quantifiable, in the case of $\text{Th}_{0.9}\text{Ce}_{0.1}\text{O}_2$. The bulk diffusion was inferred from a small long-term linear increase in gas-phase light-isotope concentration. The slow increase was not observed for exchange over thoria but as noted over doped thoria. Bulk oxygen was defined as oxygen that does not participate in the exchange at the surface.

Fischer–Tropsch Reactions

Experiments were performed with 2 : 1, 2.5 : 1 and 3 : 1 H_2 –CO gas mixtures in the 20 Torr pressure regime over the pure and doped catalysts at 685 K in order to compare their efficacy. Several factors entered the choice of these condi-

tions: to ensure that reaction would be slow enough to be compatible with the available rate of data acquisition and signal averaging; to ensure that the gas transport in the reactor was fast compared with the surface rates, *i.e.* that the observations were not diffusion limited; to ensure that the temperature was in the middle of the range over which Colmenares and McLean² reported a switch from methanol production to hydrocarbon production on thoria; and to be within the temperature range over which the oxide surface had been characterized by oxygen-isotope exchange.

Room-temperature blank experiments were run on all three types of gas mixtures because of the residual hydrocarbon impurities in the input gases and because conversion to products reached ppm concentrations only. Fig. 3 shows typical data obtained for higher-level signals. These results were obtained over ceria-doped thoria. Prior to analysis of the reaction data, the raw signal for each mass number had the corresponding background signal scaled to match initial temperature and pressure and then subtracted from the reaction signal as illustrated in Fig. 4.

The oxides, either those from an oxygen roast or those pretreated with synthesis gas, when exposed to synthesis gas, exhibited no measurable hydrocarbon production for 10–20 min, as shown in Fig. 4. Thoria or ceria-doped thoria without CO pretreatment tended to loose gas-phase CO_2 over an 80 min period when the CO_2 was present at 70–80 ppm in the 15–20 Torr feedstocks. This behaviour is illustrated in Fig. 5 (a), (c). Thoria or ceria-doped thoria that had received pretreatment with synthesis gas of feedstock composition at 15–20 Torr showed an apparent equilibrium behaviour for CO_2 . This is illustrated in Fig. 5 (b), (d). Only qualitative information could be extracted from the generation of carbon dioxide or water during the hydrocarbon induction interval because of the unknown extent of their adsorptive retention on the catalyst. Feedstocks at 100 Torr pressure and carried to larger CO conversion achieved during 13–16 h reaction showed net CO_2 release to the gas phase.

The repeated pretreatment with synthesis gas was necessary to activate the catalysts toward hydrocarbon synthesis. Presumably this treatment removed surface-bound water remaining from the preparation of the oxides, water that blocked active sites, and/or the pretreatment generated additional active sites. Also, it was found that pretreatments with H_2 alone did not suffice to activate the catalysts to hydrocarbon production. Only H_2 and CO in unison was effective in

Table 1 Oxygen isotope-exchange rates

k_1 /molecule m $^{-2}$ Pa $^{-1}$ s $^{-1}$	k_2 /molecule m $^{-2}$ Pa $^{-1}$ s $^{-1}$
present work (680–774 K)	
ThO_2	
1.66×10^{19} $\exp[(-83.3 \text{ kJ mol}^{-1})/RT]$	9.98×10^{21} $\exp[(-137 \text{ kJ mol}^{-1})/RT]$
$\text{Th}_{0.9}\text{Ce}_{0.1}\text{O}_2$	
7.05×10^{16} $\exp[(-44.0 \text{ kJ mol}^{-1})/RT]$	1.18×10^{20} $\exp[(-98.7 \text{ kJ mol}^{-1})/RT]$
Winter ¹⁵	
ThO_2 (590–690 K)	
3.27×10^{19} $\exp[(-92 \text{ kJ mol}^{-1})/RT]$	<i>ca.</i> 0
CeO_2 (720–790 K)	
2.30×10^{20} $\exp[(-109 \text{ kJ mol}^{-1})/RT]$	<i>ca.</i> $8k_1$

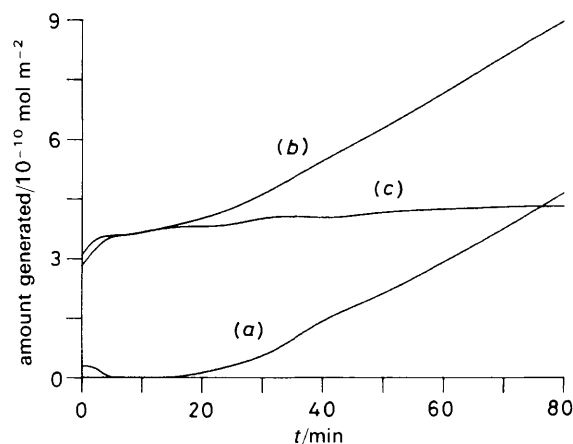


Fig. 3 Mass 15 signals. Mass spectrometer signals reported as amount generated per unit area of catalyst; feed, 2 : 1 H_2 –CO; catalyst, $\text{Th}_{0.9}\text{Ce}_{0.1}\text{O}_2$; $T = 685$ K; (a) difference signal, (b) signal and background, (c) background. The traces shown are smoothed data for one mass number selected from 60 multiplexed masses. The data density is 1 point min $^{-1}$. See text for scaling and differencing

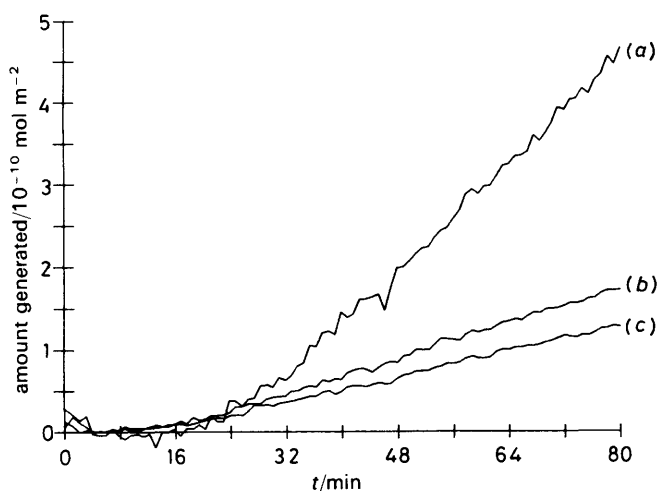


Fig 4 Mass 15, (a); 39, (b); 41, (c) production. Mass spectrometer signals reported as amount generated per unit area of catalyst; Feed, 2 : 1 H_2 -CO; catalyst, $\text{Th}_{0.9}\text{Ce}_{0.1}\text{O}_2$; $T = 685 \text{ K}$; (a), the signals were determined simultaneously at appropriate amplifier gains but are displayed on a common scale for illustration. The traces shown are unsmoothed data for each of the three mass numbers selected for illustration from 60 multiplexed signals. See text for scaling and differencing

preparing an active catalyst surface. This behaviour suggests a necessary formation of formyl- or carbonate-like precursors. Alternating H_2 and CO treatments were not attempted.

Pressure vs. time data for selected mass numbers obtained during experiments with gas mixture 2 : 1 in H_2 -CO over thoria are given in Fig. 3 and 4. Fig. 3 shows data for mass 15 in 2 : 1 H_2 -CO over $\text{Th}_{0.9}\text{Ce}_{0.1}\text{O}_2$. Fig. 3 also illustrates the background correction through a display of the raw data for mass 15 prior to blank subtraction, and the blank data on the same graph. The signals have been scaled by assuming that the sensitivity for each peak matches the sensitivity of the mass spectrometer for CO. This assumption, while rigorously incorrect, allows an analysis of the relative rates of product formation. The ionization cross-section of hydrocar-

bons relative to CO is known not to vary by more than a factor of two from one hydrocarbon to the next.

The rate of product formation was determined from the linear regions of the most prominent signals and used to compile partial cracking patterns for each experiment. These cracking patterns are the superpositions of the cracking patterns of each of the molecules in the mass spectrometer.

The spectra (cracking patterns) were decomposed into sums of molecular mass spectra by a least-squares method. Basis spectra were obtained on pure hydrocarbons in the same apparatus when those chemicals were available. Spectra for unavailable compounds were taken from the UTI 100C manuals, or from the general literature¹⁶ at 70 eV electron-impact ionization energy. Reference spectra from literature sources were compared with spectra taken in the laboratory and found to vary by not more than $\pm 10\%$ for each peak.

Table 2 details results for the rates of product formation gained from the spectral decomposition of the cracking patterns. The resulting kinetic data did not permit fitting to a phenomenological rate law, e.g. $r_i = k_i [P_{\text{CO}}]^{\alpha} [P_{\text{H}_2}]^{\beta}$.

A direct comparison between the ThO_2 and $\text{Th}_{0.9}\text{Ce}_{0.1}\text{O}_2$ catalysts was made in the 2 : 1 H_2 -CO experiment. These experiments were performed with solid samples of nearly identical surface area and with gases at the same total pressure and composition enabling a direct comparison of rates. A ratio of the rates of formation of the product hydrocarbons over each catalyst provides a simple comparison. Examination of Table 2 shows that the rate of CO conversion as determined experimentally was 3.8 times faster for the cerium-doped catalyst than for the pure thoria. The calculated rates of CO consumption were determined from the sums of the rates of production for each carbon-containing product, multiplied by the number of carbons in that product.

In every experiment, there was an induction time of approximately 15 min before a significant hydrocarbon signal could be discerned. While the specific time delay varies from mass number to mass number, the set of delays average to approximately 15 min for either of the catalysts. Because each sample was evacuated to $< 1 \times 10^{-5}$ Torr prior to the start of an experiment, the induction time was attributed to a period during which surface-bound precursors were formed and converted into desorbable hydrocarbons. The overall rates of product formation were very slow because of the low pressures (17–25 Torr) at which the observations were made. The results were therefore reflective of the state of the surface at a very early stage of the overall conversion, a stage that would be unobservable at conventional FT operating pressures of 1–30 atm of synthesis gas.

The production data contained in Table 2 shows that ThO_2 under gas mixtures used is just $> 50\%$ selective for propane and that the small amount of butene formed was but-1-ene. The data were typical for various samples examined. The $\text{Th}_{0.9}\text{Ce}_{0.1}\text{O}_2$ catalyst makes propene and propane in approximately equal proportions, but the butene was but-2-ene. Significant amounts of ethene were also produced. These changes in product distributions are reflective of changes in the sites on which intermediates were formed caused by cerium doping.

A ratio of 2.5 was calculated for CO conversion rate obtained over $\text{Th}_{0.9}\text{Ce}_{0.1}\text{O}_2$ vs. the rate obtained over ThO_2 . The 70% agreement between calculated and experimental CO conversion rates indicates that the spectral decomposition as regards to the rates of formation for each carbon number are probably correct to within $\pm 30\%$. The overall behaviour shows the cerium-doped catalyst to be superior to the undoped catalyst for achievement of conversion of CO under the present conditions.

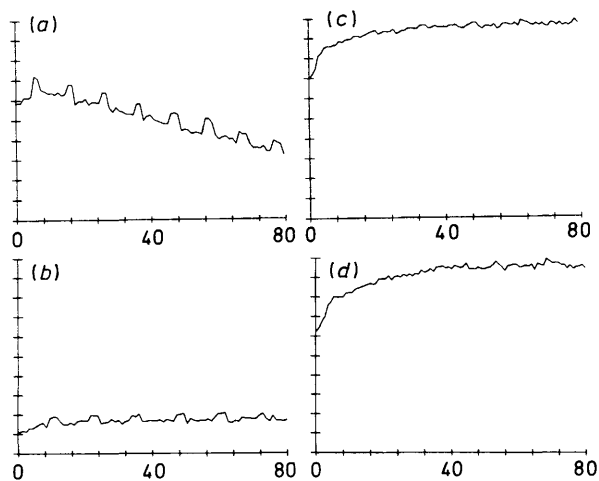


Fig. 5 CO_2 behaviour. Unsmoothed data relative to Ne tracer over O, 80 min. (a) $\text{Th}_{0.9}\text{Ce}_{0.1}\text{O}_2$, 18 Torr total pressure, initial CO_2 70 ppm, no pretreatment; (b) as (a) with H_2 -CO pretreatment; (c) ThO_2 , 17 Torr total pressure, initial CO_2 70 ppm, H_2 pretreatment; (d) as (c), H_2 -CO pretreatment. The periodic effects are associated with range changing to the most sensitive range required for following CO_2

Table 2 Product distribution 2 : 1 H₂-CO, catalysts of equal surface areas, 685 K

conditions	ThO ₂	Th _{0.9} Ce _{0.1} O ₂
initial pressure CO ^a	6.42	6.29
initial pressure H ₂ ^a	12.85	12.60
time average pressure CO ^a	6.15	5.07
time average pressure H ₂ ^a	11.10	10.14

product molecule	production rate /10 ¹² mol m ⁻² s ⁻¹		percentage of total product	
	ThO ₂	Th _{0.9} Ce _{0.1} O ₂	ThO ₂	Th _{0.9} Ce _{0.1} O ₂
CH ₄	3.30	19.9	26.3	49.9
HCCH	0.35	0.065	2.8	0.2
C ₂ H ₄	—	3.63	—	9.1
CH ₃ CHCH ₂	0.85	5.79	6.8	14.6
C ₃ H ₈	7.03	7.09	56.1	17.8
CH ₃ CH ₂ CHCH ₂	0.999	—	8.0	—
CH ₃ CHCHCH ₃	—	3.32	—	8.4
C ₁	3.30	19.9	26.3	49.9
C ₂	0.35	3.70	2.8	9.3
C ₃	7.88	12.9	62.9	32.4
C ₄	0.999	3.32	8.0	8.4
CO (expt.)	-26.6	-100		
CO (calc.)	-31.6	-79.3		
CO ₂ ^b	decreasing	decreasing	(no CO, H ₂ pretreatment)	
CO ₂ ^b	quasi-equi.	quasi-equi.	(pretreatment with CO, H ₂)	

^a Torr. ^b See text.

No oxygenated products were detected during any of the present experiments, even though the temperature of 685 K was chosen to ensure a significant yield of methanol according to earlier results.² In the earlier work a copper-lined reactor operated at low conversion was used and the thoria contained residual alkali metals from carbonate precipitation. Copper is well known as a methanol catalyst¹² and a specially active copper junction geometry is now implicated as important in reduced copper-metal oxide systems.⁹ The observations made in a copper-lined reactor may have received contributions from those factors. The current work was undertaken in a silica reactor which was verified as inert to FT synthesis under the present conditions. Because the current observations were made at low pressures, at small conversion, and using high-purity catalysts; the main results indicate that ThO₂ alone is not an intrinsic methanol catalyst.

Iso-C₄ hydrocarbons, a significant aspect of Colmenares and McLean's² work were not detected. The current data indicate that both thoria and ceria-thoria catalysts generated small (*ca.* 8%) quantities of linear butenes, as demonstrated by small mass-spectrometer signals that were a factor of three above the noise limit of the experiment. The presence of iso-C₄ at lower levels is possible, but clearly no large proportion of iso-C₄ was generated.

Discussion

Cerium-doped thoria (9 : 1 Th-Ce) has been shown to support faster rates of oxygen exchange between gas and solid, and faster rates of CO hydrogenation, than pure ThO₂. The rate-constant ratios for oxygen exchange at 685 K were $k_1(\text{Th}_{0.9}\text{Ce}_{0.1}\text{O}_2) : k_1(\text{ThO}_2) = 4.2$ for single O-atom exchange and $k_2(\text{Th}_{0.9}\text{Ce}_{0.1}\text{O}_2) : k_2(\text{ThO}_2) = 9.9$ for dioxygen exchange. In fact, $k_2(\text{Th}_{0.9}\text{Ce}_{0.1}\text{O}_2)$ was the same order of magnitude as $k_1(\text{ThO}_2)$ at 685 K. Clearly, surface oxygen in the oxide was made far more labile by cerium doping. Using the exchange rate constant for CeO₂ from Winter¹⁴ and

either our own or Winter's constant for thoria leads to the conclusion that the doped material exchanges oxygen at a much higher rate than would be expected for a simple physical mixture. This indicates that there was a cooperative interaction between the cerium and thorium ions in the doped lattice. X-Ray evidence shows that the mixed oxide system was a single-phase material in the bulk.⁷

The doped material exchanged faster than thoria and also displayed evidence of bulk diffusion, even though fewer oxygen layers participated in the exchange with gas for Th_{0.9}Ce_{0.1}O₂ than for ThO₂. The activation energies for k_1 and k_2 in the doped material were lowered by essentially the same amount, 40 kJ mol⁻¹, relative to the activation energies for those processes on ThO₂.

The doped material was faster by a factor of 3 ± 0.9 for overall CO consumption in the FT synthesis at 685 K, under otherwise identical conditions. The enhancement of the rate of hydrocarbon production by cerium doping was nearly the same as the enhancement of single O-atom exchange. That observation suggests a relation between single-atom oxygen vacancies and the rate of CO conversion. A similar relation is also evident in the work of Arai *et al.*¹⁰ on pure CeO₂. There were variations in the product distributions for each catalyst, but the rates over Th_{0.9}Ce_{0.1}O₂ were faster overall and within every carbon number relative to ThO₂. Neither catalyst produced detectable amounts of oxygenated hydrocarbon but the Ce-doped catalyst displayed a distinct tendency to form olefins preferentially to saturated hydrocarbons. A preference for formation of alkenes, particularly ethene, was also reported by Aria *et al.*¹⁷ for catalysis on In₂O₃ doped CeO₂. In this case the pressure was 25 times greater than in the present work.

Frost⁹ has proposed a junction effect between small (*ca.* 1 nm) metallic particles and surrounding metal-oxide support to explain the reduction of CO by H₂ with metal-metal-oxide based methanol catalysts. He has demonstrated that the presence of finely dispersed metal particles greatly enhances the rate of methanol synthesis over thoria. There was no measurable alcohol synthesis in the present study using high-purity

starting materials. This observation implies that alcohol synthesis on thoria requires the presence of redox couples on the oxide surface.

Mazanec⁸ has proposed a mechanism for higher alcohol synthesis from CO and H₂ over metal oxides. His arguments depend on a number of factors from the chemistry of organometallic thorium and zirconium compounds. Essentially, the mechanism requires the formation of a metal formyl by CO insertion into a surface metal hydride bond. Chain building occurs by conversion of the metal formyl to a cyclic acyl by CO insertion at the formyl carbon. The cyclic acyl undergoes a 1,2-shift of hydrogen to form an important ene-diolate intermediate. The reaction proceeds by hydrogen additions and CO insertions into the ene-diolate. Final hydrogen addition(s) result in desorbing either an alcohol or a hydrocarbon. The important intermediate is the relatively stable ene-diolate.

In the present work either pure or oxide-doped materials were used so that metallic impurity species were not present to form a metal-metal-oxide junction and provide redox properties. However, charge-compensated oxygen vacancies formed in them are proposed to provide the redox properties. A similar interpretation was presented for CO reduction on CeO₂ alone and was supported by XPS observation of a reduced but non-metallic cerium species.¹⁰ In addition to providing redox properties, the oxygen vacancies provide strong oxygen-acceptor sites. We conjecture that the weak reducing atmosphere, at 0.3% of the pressure in Frost's work is unable to displace the oxygenated intermediates at a measurable rate, as proposed by Mazanec. Instead, a reduction of the hydrocarbon at the oxygenated carbons is proposed to allow the surface complex to be desorbed, leaving behind an oxygen which heals the vacancy.

The oxygen-exchange results indicate that the cerium in the doped catalyst is very highly dispersed, thereby preventing a junction effect developing from microclusters of Ce^{III} oxide or reduced cerium metal. The greater reactivity of the cerium-doped material is attributed to its polyvalent +3/+4 character which would stabilise point oxygen vacancies. The net result should be a more-reducible surface compare with native thoria achieved by the addition of charge-compensating sites centred on the Ce ions.

Zaki and Sheppard¹⁸ have studied the surface chemistry of ceria by examining its reactivity with isopropyl alcohol. The disproportion of isopropyl alcohol *via* decomposition to acetone and then methane and isobutane was explained by mechanisms which invoke the polyvalent III/IV chemistry of cerium. It was therefore reasonable to assume that similar redox chemistry may be expected from isolated ceriums in the Th_{0.9}Ce_{0.1}O₂ experiments.

The cerium-doped material has a qualitatively measured, but clearly greater, tendency to form alkenes, particularly C₂H₄, than does ThO₂. This also supports the Mazanec ene-diolate intermediate. If Ce³⁺ is present in the structure of the ene-diolate, this could supply an electron by oxidising to Ce⁴⁺ when the intermediate is desorbed, effectively reducing the ene-diolate intermediate to an olefin. Fig. 6 illustrates how a nearby Ce^{III} ion could affect Mazanec's mechanism. That olefins would be favoured on the cerium-doped oxide relative to ThO₂ is consistent with this modification. There is no reason to assume that the CO conversion mechanism was fundamentally different on either of the two fluorite lattice materials excepting the easier availability of oxygen vacancies for the doped material.

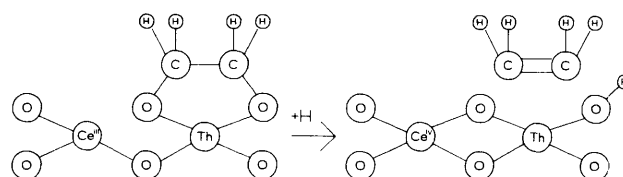


Fig. 6 Proposed mechanistic step. The important ene-diolate eliminates an olefin and heals an oxygen vacancy stabilised by Ce^{III}/Ce^{IV} redox chemistry. See text for prior steps

The resolution of an observable time delay of *ca.* 15 min between exposure to reactant and hydrocarbon appearance over these materials was achieved. Under the conditions used in this study the time delay is to be associated with stepwise formation of surface intermediates that evolve until desorbable products are created. Perhaps the time delay also occurs while a critical concentration of vacancies are formed. Although such induction periods are implicit in the early stages of FT synthesis, this work is unique in observation of that period and illustrates how closely one can approach the chemistry of the native oxide surface with selected experimental procedures.

It would be of interest to make comparisons to Zr-doped catalysts. The conclusions drawn here predict that Th-ZrO₂ catalysts would perform similarly to cerium-doped thoria, since Zr is a d²s² metal like Th and Ce, but has stable formal oxidation states of +2, +3 and +4. It is apparent that pristine oxide catalysts can behave very differently from intentionally or unintentionally promoted catalysts for what appear to be simple reasons. Among these being the junction effect, the reducing strength of the catalytic atmosphere, and the redox chemistry of the catalyst surface.

References

- 1 H. Pichler, *Adv. Catal.*, 1952, **4**, 231.
- 2 C. A. Colmanares and W. McLean, in *Development of a Demonstration Reactor using Thoria as a Fischer-Tropsch Catalyst*, Lawrence Livermore National Laboratory, Dec. 1981, Nat. Tech. Infor. Serv. Dept. of Commerce, 5285 Port Royal Road, Springfield, Va. 22161
- 3 J. Lamotte and J-C. Lavalley, *J. Chem. Soc., Faraday Trans. 1*, 1983, **79**, 2219.
- 4 J. Lamotte, J-C. Lavalley, V. Lorenzelli and E. Freund, *J. Chem. Soc., Faraday Trans. 1*, 1985, **81**, 215.
- 5 G. Busca, J. Lamotte, J-C. Lavalley and V. Lorenzelli, *J. Am. Chem. Soc.*, 1987, **109**, 5197.
- 6 A. Grabbe, Ph.D. Thesis, University of North Carolina at Chapel Hill, 1989.
- 7 H. J. Whitfield, D. Roman and A. R. Palmer, *J. Inorg. Nucl. Chem.*, 1966, **28**, 2817.
- 8 T. J. Mazanec, *J. Catal.*, 1986, **98**, 115.
- 9 J. C. Frost, *Nature (London)*, 1988, **334**, 577.
- 10 T. Arai, K. Maruya, K. Domen and T. Onishi, *Chem. Lett.*, 1989, 47.
- 11 M. Breyse, *Ann. Chim.*, 1967, **2**, 370.
- 12 W. S. Brey and B. H. Davis, *J. Colloid. Interface Sci.*, 1979, **70**, 10.
- 13 K. Klier, J. Novakova and P. Jiru, *J. Catal.*, 1963, **2**, 479.
- 14 E. R. S. Winter, *Adv. Catal.*, 1958, **10**, 196.
- 15 J. Novakova, *Catal. Rev.*, 1970, **4**, 77.
- 16 E. Stenhagen, S. Abrahamsson and F. W. McLafferty, *Registry of Mass Spectral Data*, Wiley, New York, 1974. vol. 1.
- 17 T. Arai, K. Maruya, K. Domen and T. Onishi, *Bull. Chem. Soc. Jpn.*, 1989, **62**, 349.
- 18 M. I. Zaki and N. Sheppard, *J. Catal.*, 1983, **80**, 114.